Journal of Applied Mechanics and Technical Physics, Vol. 51, No. 1, pp. 137–144, 2010

FORMATION OF A SPALL CAVITY IN A DIELECTRIC DURING ELECTRICAL EXPLOSION

V. V. Burkin, N. S. Kuznetsova, and V. V. Lopatin

UDC 537.529+534.222.2

The wave dynamics of the stress–strain state of a solid dielectric during electrical explosion near its surface is analyzed. A quantitative model of an electrical explosion is developed which describes the operation of a high-voltage generator, the expansion of the discharge channel, and the generation and distribution of shock-wave perturbations. Two mechanisms of formation of a spall cavity on the surface of the solid are considered: the less energetic mechanism implemented by means of the waves reflected from the surface, and the more energetic mechanism in which result from the action of a direct wave of compressive stresses. The effects of the reflection surface shape and the mode of energy input into the channel on the possible fracture pattern are estimated.

Key words: *electrical explosion, shock-wave perturbations, spall cavity, mechanical stresses.*

Introduction. Under certain conditions, pulse breakdown of solid dielectrics connected to electrodes and immersed in a liquid (Fig. 1) exhibit the Vorob'ev effect [1], in which the moving discharge channel penetrates into the solid dielectric [2–4]. The penetration of the channel into a solid dielectric or semiconductor material is determined by the electrical conductivities and polarities of the liquid and solid, the ratio of the impedances of the high-voltage generator to the discharge gap and occurs at a high voltage rise rate when the delay of a breakdown of about several centimeters is less than 10^{-6} sec [2, 3]. The voltage pulse applied to the electrodes initiates growth of discharge channels from the anode mainly along the liquid–solid interface [3]. At a distance from the surface of the solid equal to 0–$S/4$ (S is the distance between the electrodes) [2], one of the channels propagates into the solid dielectric and closes the gap due to the high propagation velocity: $V_s/V_{liq} \approx 1.5$–10.0 (V_s and V_{liq} are the velocities of propagation of the discharge channels in the solid and liquid, respectively) [5–7]. It is agreed that, under optimal conditions, the penetration depth of the channel is $h \approx (1/4$–$1/3)S$ [2].

The destructive action of a pulse discharge in solids (electrical explosion) whose surfaces are connected to electrodes is used in borehole drilling [2, 8], desurfacing, and cutting [9]. Quantitative fracture characteristics, except for the characteristics of prebreakdown phenomena during channel penetration into a solid, are determined by energy transfer to the channel plasma, shock-wave generation by the expanding channel, wave dynamics in the presence of the solid–liquid interface, and the formation of the stress–strain state of the medium leading to fracturing. Compared to fracture by a through breakdown path, in the case of cylindrical symmetry [10–12], the presence of a nearby interface between two media should lead to changes in wave dynamics and, hence, fracture characteristics of the near-surface material, and possibly, spallation mechanism. The purpose of the present work is to develop a quantitative two-dimensional model for the formation of a spall cavity by a discharge channel penetrating into the solid and to analyze the fracture mechanisms for various energy input conditions. The development of such a model is important for the choice and optimization of parameters of technological pulse generators.

Physicomathematical Model of Wave and Deformation Processes. The discharge channel about 5–10 μm [13] in diameter formed in the prebreakdown stage and heated by the discharge current of the energy storage expands in 10^{-6}–10^{-4} sec and generates a mechanical stress wave into the surrounding material. Near

High Voltage Research Institute, Tomsk Polytechnic University, Tomsk 634050; tevn@hvd.tpu.ru. Translated from Prikladnaya Mekhanika i Tekhnicheskaya Fizika, Vol. 51, No. 1, pp. 162–172, January–February, 2010. Original article submitted July 25, 2008; revision submitted January 26, 2009.

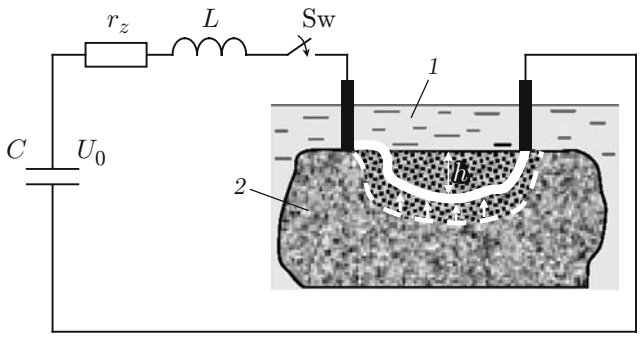

Fig. 1. Diagram of fracture of a solid dielectric under an electric discharge: 1) water; 2) solid (h is the depth of penetration of the channel); C is the storage capacity, U_0 is the charge voltage, r_z and L are the resistance and inductance of the discharge circuit, respectively, and Sw is the switch.

the channel, the wave degenerates into a plastic deformation region and an elastic wave which propagates to the periphery. Wave formation in solids during electrical explosion has been investigated in detail [11, 12].

When the wave generated by the channel reaches the boundary with the liquid, the wave is partially reflected into the solid and refracted

into the liquid. The wave refracted into the liquid is much weaker than the wave reflected into the solid. The energy transferred by this wave to the liquid is less than 1% of the energy accumulated in the storage; therefore, it can be ignored in the analysis [11]. This assumption is valid for a solid–liquid system in which the wave propagation velocity is much higher in the solid than in the liquid. At a channel penetration depth approximately equal to 5–10 mm, the reflected wave propagating in the solid at a velocity of about 4–6 km/sec travels this distance in time $t < 2.5$ μsec. In the same time, the wave refracted into the liquid (for example, water) travels a distance less than 4 mm. Taking into account the aforesaid and the considerable difference in acoustic impedance between the neighboring media, the energy transferred to the liquid in the time interval considered can be ignored because it is low compared to the energy accumulated in the solid [14].

The solution of the problem (modeling of the spall cavity during electrical explosion) is a two-dimensional model that allows one to perform computer experiments with electrical explosion in solids. In electrical explosion, the reflected and direct waves interfere. Computer experiments have shown that, for values of $h \approx 5$–10 mm obtained in physical experiments [2], the interference is manifested as anisotropy of the stress–strain state of the material in radial sections located along the beams which deviate from the normal to the surface by an angle approximately equal to 60° (section Cr in Fig. 2a). In these sections, the tensile radial stresses σ_r in the reflected wave are summed with the tangential tensile stress σ_t in the direct wave. As a result, the most favorable conditions for the formation of radial cracks forming a spall cavity in the material (see Fig. 2) are produced in the vicinity of these sections.

The model equations of the electrical explosion include relations for electrotechnical parameters, energy release in the plasma channel, and wave dynamics in the solid dielectric.

The Kirchhoff equations

$$L\,\frac{di}{dt} + (r_z + R_{\rm ch})i = U, \qquad \frac{dU}{dt} = -\frac{i}{C} \tag{1}$$

with the initial conditions $i(0) = 0$ and $U(0) = U_0$, where U_0 is the charge voltage, allow one to calculate the circuit current strength $i(t)$, the channel resistance $R_{\rm ch}(t)$, and the energy release dynamics in the channel $W_{\rm ch}(t)$:

$$W_{\rm ch}(t) = \int\limits_0^t i^2(t) R_{\rm ch}(t)\,dt. \tag{2}$$

The resistance of the breakdown path was determined through the current action integral using the relation [15]

$$R_{\rm ch}(t) = K l_{\rm ch} \Big/ \Big(\int\limits_0^t i^2(t)\,dt \Big)^{1/2}, \tag{3}$$

where K is a coefficient that characterizes the dielectric [16].

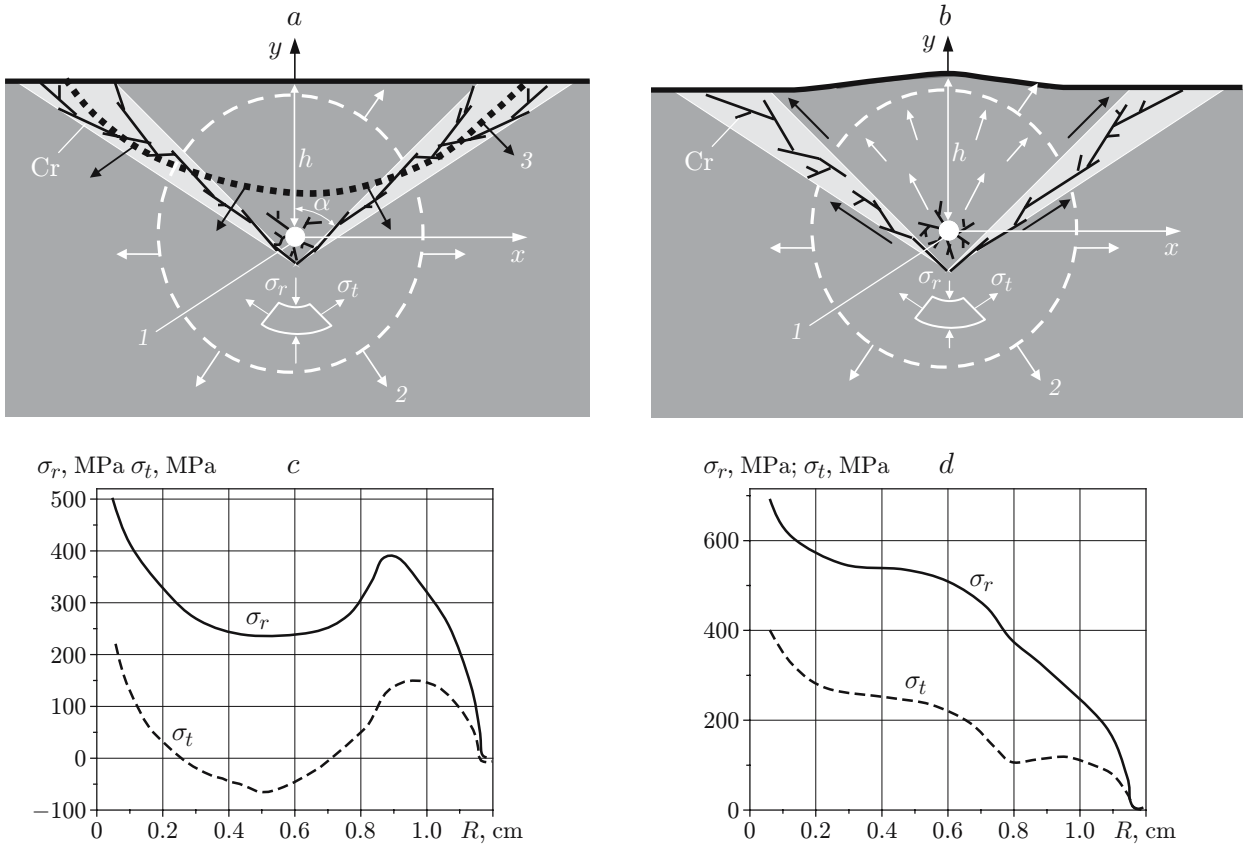

Fig. 2. Cross sections of the discharge channel (a and b) and stress profiles in the wave in the sections Cr (c and d) at the time $t = 1.7$ μsec at $h = 6$ mm: (a, c) rapid energy input ($W_{\text{g}} = 118$ J and $T = 0.46$ μsec); (b, d) slow energy input ($W_{\text{g}} = 588$ J and $T = 1.33$ μsec); 1) breakdown channel; 2) direct wave; 3) wave reflected from the surface; areas of the most probable crack formation are denoted as Cr.

According to [17], in Cartesian coordinates with the ordinate axis perpendicular to the reflection surface and the abscissa axis parallel to the surface layer and perpendicular to the channel axis, the problem of plane deformation of an elastoplastic material includes:

— the equations of motion

$$\frac{\partial \sigma_{xx}}{\partial x} + \frac{\partial T_{xy}}{\partial y} = \rho \ddot{x}, \qquad \frac{\partial T_{xy}}{\partial x} + \frac{\partial \sigma_{yy}}{\partial y} = \rho \ddot{y},$$
$$\sigma_{xx} = S_{xx} - P, \qquad \sigma_{yy} = S_{yy} - P, \qquad \sigma_{zz} = S_{zz} - P; \tag{4}$$

— the continuity equation

$$\frac{\dot{V}}{V} = \frac{\partial \dot{x}}{\partial x} + \frac{\partial \dot{y}}{\partial y}, \qquad V = \frac{\rho_0}{\rho}; \tag{5}$$

— the equation of internal energy of the medium

$$\dot{e} = -P\dot{V} + V(S_{xx}\dot{\varepsilon}_{xx} + S_{yy}\dot{\varepsilon}_{yy} + T_{xy}\dot{\varepsilon}_{xy}); \tag{6}$$

— the relations for the components of the stress deviator S_{ij} and strain rates $\dot{\varepsilon}_{ij}$

$$\dot{S}_{xx} = 2\mu\Big(\dot{\varepsilon}_{xx} - \frac{1}{3}\frac{\dot{V}}{V}\Big), \qquad \dot{S}_{yy} = 2\mu\Big(\dot{\varepsilon}_{yy} - \frac{1}{3}\frac{\dot{V}}{V}\Big), \qquad \dot{S}_{zz} = -\frac{2}{3}\mu\frac{\dot{V}}{V}, \qquad \dot{T}_{xy} = \mu\dot{\varepsilon}_{xy},$$
$$\dot{\varepsilon}_{xx} = \frac{\partial \dot{x}}{\partial x}, \qquad \dot{\varepsilon}_{yy} = \frac{\partial \dot{y}}{\partial y}, \qquad \dot{\varepsilon}_{xy} = \frac{\partial \dot{y}}{\partial x} + \frac{\partial \dot{x}}{\partial y}; \tag{7}$$

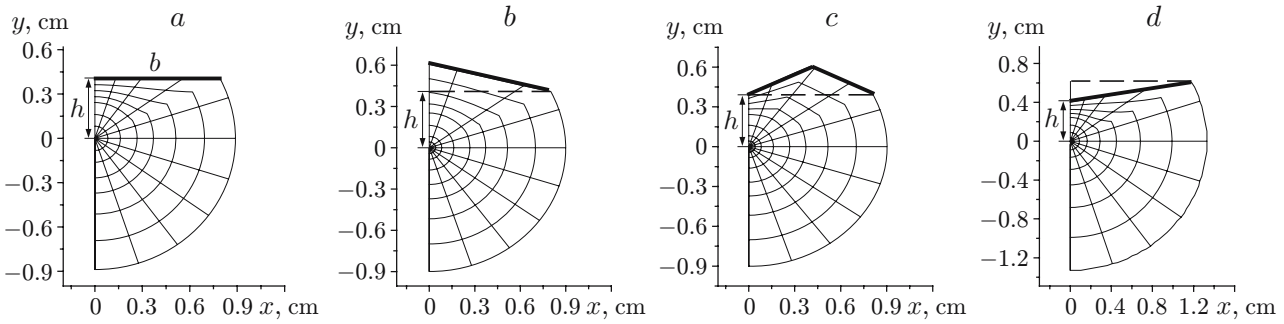

Fig. 3. Shapes of computation domains.

— the Mises yield condition

$$S_{xx}^2 + S_{yy}^2 + S_{zz}^2 + 2T_{xy}^2 \leqslant 2Y^2/3. \tag{8}$$

In (4)–(8), x and y are Cartesian coordinates, $\dot{x}$, $\dot{y}$, $\ddot{x}$, and $\ddot{y}$ are the velocities and accelerations along the corresponding axes, σ_{xx} and σ_{yy} are the total stresses acting in the areas perpendicular to the OX and OY axes, respectively, σ_{zz} is the total stress acting in the areas perpendicular ho the channel axes, T_{xy} is the shear stress, P is the pressure, e is the internal energy of unit mass, V is the relative volume, ρ_0 and ρ are initial and current densities, and μ and Y are the shear modulus and yield point of the material; dot denotes differentiation with respect to time.

The initial conditions for the material was the unperturbed state:

$$\dot{x} = 0, \qquad \sigma_{xx}(x,y) = 0, \qquad \sigma_{yy}(x,y) = 0, \qquad \sigma_{zz}(x,y) = 0,$$

$$T_{xy}(x,y) = 0, \qquad \rho = \rho_0, \qquad e(x,y) = 0.$$

The boundary condition on the channel wall was the dependence $P_{\rm ch}(t)$, which, as in [11], was determined from the energy balance equation for the discharge channel

$$\frac{dW_{\rm ch}}{dt} = \frac{dA_{\rm ch}}{dt} + \frac{1}{\gamma - 1}\,\frac{d(P_{\rm ch}V_{\rm ch})}{dt}, \tag{9}$$

where $dA_{\rm ch} = P_{\rm ch}\,dV_{\rm ch}$ is the increment of the work performed by the expanding channel as its volume $V_{\rm ch} = \pi r_{\rm ch}(t)^2 l_{\rm ch}$ changes under the action of the pressure in the channel $P_{\rm ch}$; $r_{\rm ch}(t)$ is the channel radius; $W_{\rm pl} = P_{\rm ch}V_{\rm ch}/(\gamma - 1)$ is the energy of the plasma expanding in the adiabatic approximation (the value of the parameter γ was set equal to 1.1). The surface $y = h$ was considered free: $\sigma_{yy} = 0$.

The pressure in the wave was calculated using the barotropic relation [18]

$$P = \rho_0 c_{\rm liq}^2(\rho/\rho_0 - 1)(\rho/\rho_0)^n. \tag{10}$$

For $\rho_0 = 2.67$ g/cm^3, $c_{\rm liq} = 5850$ m/sec, $n = 2$, $\mu = 31.6 \cdot 10^9$ Pa, and $Y = 0.25 \cdot 10^9$ Pa, relations (1)–(7) describe the compressibility and elastic and plastic deformation of a material similar in properties to granite.

The problem was solved numerically. The electrotechnical equations were integrated by the Euler implicit method. The system of dynamic equations (1)–(10) was solved using difference schemes [17] on a two-dimensional computation grid, whose various shapes are given in Fig. 3 (b is the half-width of the reflection surface). The ordinate axis was the symmetry axis of the channel. Deviations of the channel in the near-electrode regions from a position parallel to the reflection surface were ignored. In the vicinity of the channel with the coordinates of its axis $x = 0$ and $y = 0$, the shape of the computation cells corresponded as much as possible to the cylindrical shape of the channel. Near the surface $y \approx h$, the cell shape was adapted to describe the wave reflection from the surface of the corresponding shape. The chosen parameters of the computation grid satisfied the following conditions: $b \geqslant 2h$, number of beams in the expansion angle $J = 80$–100, number of computation nodes in the radial direction $M = h/r_{\rm ch0} = 800$–100, and initial radius of the channel $r_{\rm ch0} = 5$ μm. In the calculation, these conditions provided an about 3% disbalance between the work performed by the channel and the wave energy. The numerical solution was tested using a one-dimensional version of the computation grid ($b = 0$) by comparing with

the analytical solution of the problem of expansion of a cylindrical piston in water at a constant velocity [19] under the assumption of flow self-similarity [20]. The stress–strain state in the sections Cr was analyzed using the values of the main radial σ_r and tangential σ_t stresses determined according to [17].

The proposed model was used to analyze the formation mechanism of a spall cavity during buried electrical explosion in granite with the following mechanical characteristics: $\sigma_{\text{rup}} = 7.85$ MPa, $\sigma_{\text{sh}} = 9.81$ MPa (ultimate rupture and shear stresses, respectively [21]), and average value of the spark constant $K_{\text{mid}} = 611$ V$\cdot$ sec$^{1/2}\cdot$m^{-1} [16]. The channel length was $l_{\text{ch}} = 2$ cm and $h = 4$–8 mm. The discharge circuit parameters were varied in the following ranges: $U_0 = 250$–350 kV, $C = 3$–20 nF, $L = 5$–25 μH, and $r_z = 1\ \Omega$, which corresponds to the electrical discharge modes [2] with a Marx pulse generator. By using the values of the strength criteria obtained for static conditions, one can qualitatively estimate the crack formation conditions. For a more detailed investigation of the fracture mechanisms involved in the formation of a spall cavity, it is necessary to use the dynamic laws of variation of these quantities [22].

Formation of Spall Cavities. The modeling results showed that, depending on the amount of energy, the rate of its input to the channel,and channel penetration depth h, different scenarios of wave dynamics and, hence, different material fracture mechanisms can occur. Possible patterns of interaction of the wave with the reflection surface are given in Fig. 2. The wave profile presented in Fig. 2c is formed in the mode of rapid energy input to the channel by a low-inductance generator with the half-cycle of discharge current oscillations $T \approx \pi\sqrt{LC} < 1$ μsec. In this case, near the discharge channel (at a distance $R = \sqrt{x^2 + y^2} \approx 1$–2 mm), high compressive stresses arise which form a region of material grinding. In this region, the solid dielectric is ground under the action of compressive stresses. In the region $R \geqslant 2$ mm, the tangential stresses σ_t become tensile. During wave propagation, the radius of the region of tensile stresses increases and the stresses σ_t in the wave increase upon its reflection. The reflected wave interferes with the direct wave, the stresses are summed up as a result of superposition, and the region of tensile stresses exceeding the material rupture strength occupies an increasingly larger part of the material. This interaction is most intense in the radial sections Cr (see Fig. 2a) with an expansion angle $\alpha \approx 100$–140°, in which there are the most favorable conditions for crack formation due to the resulting tensile stresses. This version of the process is analyzed using the fracture criterion $\sigma = \sigma_{\text{rup}}$.

In the case of slow energy input to the channel ($T > 1$ μsec), a region of tensile tangential stress has not formed by the moment the wave reaches the free surface. In the time interval considered, the stresses in the wave remain compressive. Under theses conditions, part of the material above the channel is displaced toward the surface. The sections Cr separating the displaced part and the motionless bulk of the material and located at an angle α to the ordinate (see Fig. 2b) are subjected to shear strain. Once the strain reaches critical values, cracks occur in these sections and the material above the channel is displaced toward the free surface. As a result, a spall cavity is formed. In this case, the material fracture is due to the shear strain caused by the largest shear stress in the direct wave. In this case, the role of the reflected waves is insignificant. Figure 4 gives calculated shear strains ε_{xy} in elements of the medium located in various sections. A comparison of the distributions ε_{xy} shows that the largest values of ε_{xy} are reached in the sections located along the radius at angles $\alpha \approx 40$–50° to the OY axis. Hence, in the case of slow energy input, cracks connecting the material grinding region near the channel to the surface are formed in exactly these sections.

In the two cases, despite differences in fracture mechanisms, the predicted transverse sizes of cavities differ only slightly. We note that, in physical experiments at $T \geqslant 1$ μsec, fracture also has the form of spallation of one or several fragments similar in shape to the spall presented in Fig. 5.

The energy parameters of material fracture during electrical explosion can be improved by optimizing the mode of energy input to the channel. To compare the energy fracture for two modes of energy input to the channel (see Fig. 2a and b), we calculated the volume of the cavity V_{cav} formed during electrical explosion and the specific fracture energy $W_{sc} = W_{\text{g}}/V_{\text{cav}}$ (W_{g} is the energy stored in the generator). The spall cavity was approximated by a triangular prism of length l_{ch} whose bases are the sections Cr formed by the planes of the most probable crack formation (see Fig. 2). The calculation results for two modes of energy input: rapid ($W_{\text{g}} = 118$ J and $T = 0.46$ μsec) and slow ($W_{\text{g}} = 588$ J and $T = 1.33$ μsec) made it possible to estimate the volume of the cavity formed: $V_{\text{cav}} \approx 0.94$ cm^3. In both cases, the channel penetration depth was $h = 6$ mm, and the cavity depth was set equal to 8 mm since the material grinding region near the discharge channel was involved in fracture. In the rapid discharge mode, the specific fracture energy was $W_s \approx 125$ J/cm^3 and in the slow mode, $W_{sc} \approx 625$ J/cm^3.

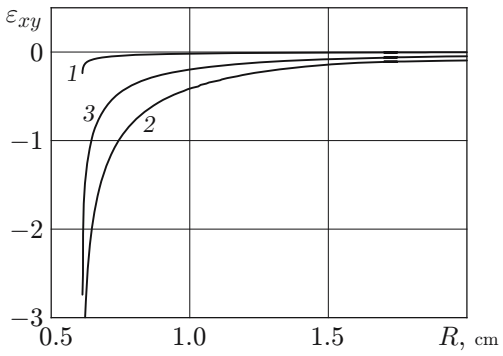

Fig. 4

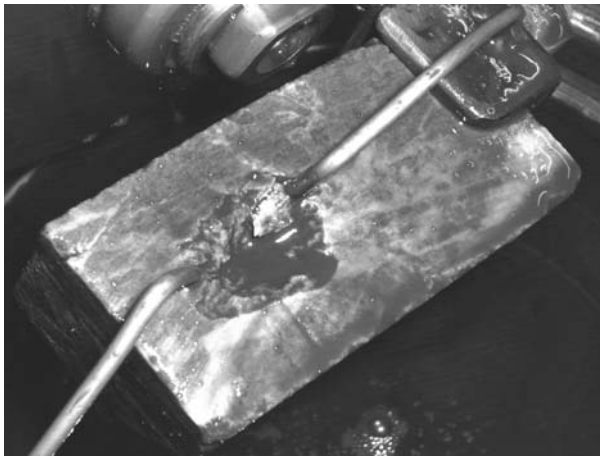

Fig. 5

Fig. 4. Shear strain versus distance R ($t = 1.7$ μsec, $h = 6$ mm, $W_{\rm g} = 588$ J, and $T = 1.33$ μsec) in sections corresponding to various values of the angle α: $\alpha = 0^\circ$ (1), 40° (2), and 70° (3).

Fig. 5. Spall cavity produced by electrical explosion in sandstone.

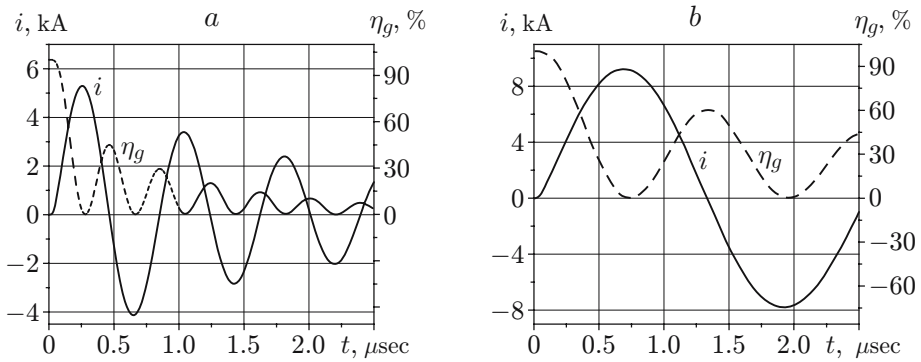

Fig. 6. Current strength i and relative energy consumption of the generating capacitor $\eta_{\rm g}$ versus time: (a) rapid energy input mode ($W_{\rm g} = 118$ J and $T = 0.46$ μsec); (b) slow energy input mode ($W_{\rm g} = 588$ J and $T = 1.33$ μsec).

The estimates obtained show that rapid modes of energy input to the channel allow one to minimize the energy consumption in fracture. The lower energy consumption of rapid discharge modes, which provide higher rate of energy input, is due to material fracture by tensile stresses, whose ultimate values are smaller than those in shear ($\sigma_{\rm rup} < \sigma_{\rm sh}$).

Another important effect of rapid energy input to the channel is the larger coefficient of transformation of the generator energy to the energy of the wave [11]. An analysis of the energy parameters shows that, in the examined range of values of C and L, only part of the storage energy is consumed by the moment wave reflection begins. Figure 6 and 7 show the variation in the current strength in the circuit, the relative energy consumption of the generating capacitor $\eta_g = CU^2(t)/(CU_0^2)$, and energy release rate in the channel for the discharge mode considered. A comparison of the current–time curves and energy characteristics of the process show that, by the moment the wave reaches the surface, the energy consumption is 30 to 90% of the storage energy, depending on the circuit parameters and the penetration depth of the channel. In the rapid discharge mode, the generator energy consumption is more rapid, and, hence, the larger part of its energy is transformed to the mechanical energy of the wave in a shorter time. In the slow mode of energy input to the channel, the larger part of the generator energy is consumed already after the establishment of the material fracture conditions, i.e., it is consumed inefficiently.

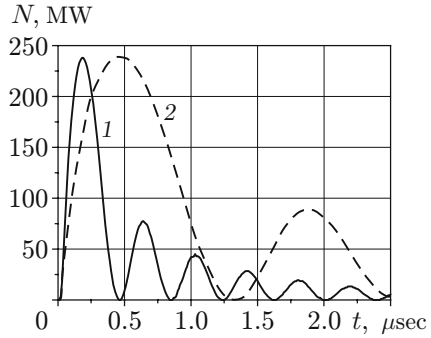

Fig. 7. Rate of energy input to the channel N versus time: 1) rapid energy input mode ($W_g = 118$ J and $T = 0.46$ μsec); 2) slow energy input mode ($W_g = 588$ J and $T = 1.33$ μsec).

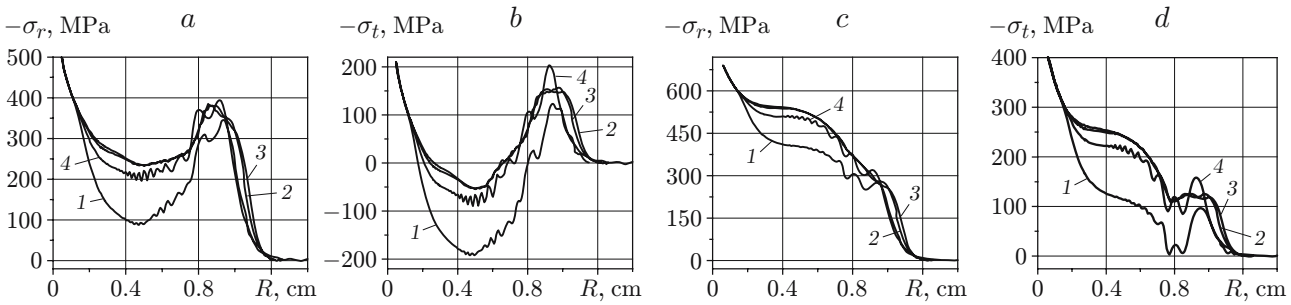

Fig. 8. Curves of the main radial σ_r (a and c) and tangential σ_t (b and d) stresses at $t = 1.7$ μsec: (a, b) $W_g = 118$ J and $T = 0.46$ μsec; (c, d) $W_g = 588$ J and $T = 1.33$ μsec; curves 1–4 corresponding to the shapes of the reflection surfaces in Fig. 3a and c.

The wave pattern in the near-surface region of the dielectric depends not only on the parameters of the wave reaching the surface but also on the shape of the reflection surface, which, in practice, is rough and uneven. In the calculations, four versions of the surface shape (see Fig. 3) were considered. By virtue of symmetry, Fig. 3 gives only the right segments of the computation domain. The typical size of the surface roughness did not exceed $h/2$. The corresponding stress curves in the sections located along the radius at angles $\alpha = 40$–$50°$ (region Cr in Fig. 2) are given in Fig. 8. The calculations performed showed that the wave dynamics calculated using the diagrams presented in Fig. 3b–d is similar in nature and differs significantly from the wave dynamics calculated using the diagram given in Fig. 3a. We note that, at a low rate of energy input to the channel (see Fig. 8c and d), cavity formation mechanism occurs at a large excess of energy in the wave and does not depend on the shape of the reflection surface. In the rapid modes of energy input to the channel, the values of the tensile tangential stress and the sizes of the corresponding regions depend on the shape of the reflection surface. This implies that the volume of the cavity formed depends on the conditions of wave reflection from the surface.

In conclusion, we note that both of the examined mechanism lead to the formation of a spall cavity which is similar in shape to the cavity shown in Fig. 5. In this case, the formation mechanisms of the spall cavity are similar to the mechanisms of the processes involved in the high-speed impact on a target [23]. If the target thickness is great enough, the wave process occurring in it results in the classical version of spall caused by tensile stresses. During the interaction of an impactor with a thin target, the formation of a hole in it is caused by shear strains.

Conclusions. The formation mechanisms of a spall cavity on the surface of a solid during electrical explosion can differ, depending on the discharge energy and the rate of its input to the channel. Rapid energy input to the channel by a low-inductance generator ($T \approx \pi\sqrt{LC} < 1$ μsec) provides the formation of a cavity due to the resulting tensile tangential stress arising from the interference of the wave incident on the free surface and the wave reflected from it in the form of a tension wave. In this case, the volume and shape of the spall cavity is affected by the conditions of wave reflection from the surface. This energy input mode provides lower energy consumption in material fracture than that in the slow mode of energy input.

In the slow mode of energy input to the channel and a small penetration depth of the channel, a spall cavity is formed due to shear strains in the direct wave. In this case, the reflected wave has a less significant effect. Accordingly, the surface shape has a negligible effect on the stress–strain state of the near-surface layer and, hence, on the cavity sizes. In the slow mode of energy input, the energy consumption in fracture is several times higher than that in the rapid energy input mode. Hence, the rapid mode of energy input to the discharge channel in the presence of a nearby surface is preferred from the viewpoint of energetic efficiency.

This work was supported by the Russian Foundation for Basic Research (Grant No. 08-08-01016-p) and the program Development of Scientific Potential of the Higher School (RNP.2.1.1.53.43).

REFERENCES

1. A. A. Vorob'ev, *Rock Breaking by Electrical Pulse Discharges* [in Russian], Izd. Tomsk. Univ., Tomsk (1961).
2. B. V. Semkin, A. F. Usov, and V. I. Kurets, *Fundamentals of Material Fracture by an Electrical Pulse* [in Russian], Nauka, St. Petersburg (1995).
3. V. T. Kazub, G. S. Korshunov, and A. T. Chepikov, "On the formation of a discharge in a system of electrodes located at the interface between liquid and solid dielectrics," *Izv. Vyssh. Uchebn. Zaved., Fiz.*, No. 9, 61–66 (1978).
4. G. A. Mesyatz, "On the nature the Vorob'evykh effect in the physics of pulse breakdown of solid dielectrics," *Pis'ma Zh. Tekh. Fiz.*, **31**, No. 24, 51–59 (2005).
5. G. Z. Usmanov, V. V. Lopatin, M. D. Noskov, and A. A. Cheglokov, "Simulation of electrical discharge development at interface of solid and liquid dielectric," *Izv. Vyssh. Uchebn. Zaved., Fiz.*, **10**, 231–234 (2006).
6. V. Ya. Ushakov, V. F. Klimkin, S. M. Korobeinikov, and V. V. Lopatin, in: V. Ya. Ushakov (ed.), *Breakdown of Liquids by a Pulsed Voltage* [in Russian], Izd. Nauch. Tekh. Lit., Tomsk (2005).
7. A. A. Vorob'ev and G. A. Vorob'ev, *Electrical Breakdown and Fracture of Solid Dielectrics* [in Russian], Vysshaya Shkola, Moscow (1966).
8. I. V. Timoshkin, J. W. Mackersie, and S. J. MacGregor, "Plasma channel miniature hole drilling technology," *IEEE Trans., Plasma Sci.*, **32**, No. 5, 2055–2061 (2004).
9. D. Jgun, M. Jurkov, V. Lopatin, et al., "Application of pulsed discharges for materials cutting," in: *Digest of Paper of Europ. Pulsed Energy Symp.*, Saint Louis, France (2002), pp. 22/1–22/4.
10. V. V. Burkin, N. S. Kuznetsova, and V. V. Lopatin, "Analysis of mechanisms of rock destruction in electro discharge drilling," *Izv. Vyssh. Uchebn. Zaved., Fiz.*, No. 11 (Append.), 507–510 (2006).
11. V. V. Burkin, N. S. Kuznetsova, and V. V. Lopatin, "Modeling of electrical explosion in solid dielectrics in electrical discharge technologies," *Izv. Tomsk. Politech. Univ.*, **309**, No. 2, 70–75 (2006).
12. V. V. Burkin, "Characteristics of the explosive action associated with the pulsed electrical breakdown of hard materials," *Combust., Expl., Shock Waves*, No. 4, 484–487 (1985).
13. Yu. N. Vershinin, *Electron-Thermal and Detonation Processes during Electrical Breakdown of Solid Dielectrics* [in Russian], Izd. Ural. Otd. Ross. Akad. Nauk, Ekaterinburg (2000).
14. V. V. Burkin, N. S. Kuznetsova, and V. V. Lopatin, "Dynamics of electrical explosion in a solid dielectric immersed in a liquid," in: *Fundamental and Applied Problems of Modern Mechanics*, Proc. 5th Al-Russian Conf. (Tomsk, October 3–5, 2006), Tomsk. Politekh. Univ., Tomsk (2004), pp. 104–106.
15. R. Rompe and W. Weizel, "Über das Toeplersche Funkengesetz," *Z. Phys. B*, **122**, 9–12 (1944).
16. B. V. Semkin, A. F. Usov, and N. T. Zinov'ev, *Transient Processes in Electric-Pulse Facilities* [in Russian], Nauka, St. Petersburg (2000).
17. M. L. Wilkins, "Calculation of elastic–plastic flow," in: B. Alder, S. Frenbach, and M. Rotenberg (eds.), *Methods of Computational Physics*, Academic Press, New York–London (1964).
18. M. Born and M. Göppert-Mayer, *Handbuch der Physik*, Springer-Verlag, Berlin (1933).
19. K. A. Naugolnykh and N. A. Roi, *Electrical Discharges in Water* [in Russian], Nauka, Moscow (1971).
20. I. Z. Okun', "Calculation of liquid pressure on a piston at a constant speed of piston expansion," *Izv. Akad. Nauk SSSR, Mekh. Zhidk. Gaza*, No. 1, Issue 1, 126–130 (1968).
21. K. P. Stanyukovich (ed.), *Physics of Explosion* [in Russian], Nauka, Moscow (1975).
22. E. N. Bellendir, V. V. Belyaev, and O. B. Naimark, "Kinetics of multifocal fracture under spalling conditions," *Pis'ma Zh. Tekh. Fiz.*, **15**, No. 13, 90–93 (1989).
23. J. A. Zukas, T. Nicholas, H. F. Swift, A. B. Greszczuk, and D. R. Curran, *Impact Dynamics*, New York, Wiley (1982).